

---

11 May 2021

## Copper Selenide as Multifunctional Non-Enzymatic Glucose and Dopamine Sensor

Harish Singh

Jillian Bernabe

Justin Chern

Manashi Nath

Missouri University of Science and Technology, nathm@mst.edu

Follow this and additional works at: [https://scholarsmine.mst.edu/chem\\_facwork](https://scholarsmine.mst.edu/chem_facwork)

 Part of the [Chemistry Commons](#)

---

### Recommended Citation

H. Singh et al., "Copper Selenide as Multifunctional Non-Enzymatic Glucose and Dopamine Sensor," *Journal of Materials Research*, Cambridge University Press, May 2021.

The definitive version is available at <https://doi.org/10.1557/s43578-021-00227-0>



This work is licensed under a [Creative Commons Attribution-Noncommercial-No Derivative Works 4.0 License](#).

This Article - Journal is brought to you for free and open access by Scholars' Mine. It has been accepted for inclusion in Chemistry Faculty Research & Creative Works by an authorized administrator of Scholars' Mine. This work is protected by U. S. Copyright Law. Unauthorized use including reproduction for redistribution requires the permission of the copyright holder. For more information, please contact [scholarsmine@mst.edu](mailto:scholarsmine@mst.edu).



# Copper selenide as multifunctional non-enzymatic glucose and dopamine sensor

Harish Singh<sup>1</sup>, Jillian Bernabe<sup>1</sup>, Justin Chern<sup>1</sup>, Manashi Nath<sup>1,a)</sup> 

<sup>1</sup>Department of Chemistry, Missouri University of Science & Technology, Rolla, MO 65409, USA

<sup>a)</sup>Address all correspondence to this author. e-mail: nathm@mst.edu

Received: 16 February 2021; accepted: 27 April 2021

**Cu<sub>2</sub>Se, synthesized through one-pot hydrothermal synthesis, was identified as highly efficient bifunctional sensor for co-detection of glucose and dopamine with high selectivity. As-synthesized copper selenide could electro-oxidize glucose and dopamine at different applied potentials. Glucose oxidation was observed at 0.35 V while dopamine oxidized at 0.2 V. This copper selenide-based non-enzymatic sensor showed high sensitivity for both glucose (15.341 mA mM<sup>-1</sup> cm<sup>-2</sup>) and dopamine (12.43 μA μM<sup>-1</sup> cm<sup>-2</sup>) with low limit of detection (0.26 μM and 84 nM). Such high sensitivity and low LOD makes this sensor attractive for possible detection of glucose/dopamine in physiological body fluids which have low concentration of these biomolecules. Extremely low applied potential for detection also makes it ideal for integrating into wearable continuous monitoring devices with low operational power requirement. This sensor showed high reproducibility, reusability and long-term operational stability along with high degree of selectivity for dopamine and glucose sensing in presence of other interferents.**

## Introduction

Diabetes and neurodegenerative diseases have continued to be one of the major causes of death affecting millions of people globally. One of the major treatment modules for these diseases is to keep progression of the disease under check by monitoring the respective biomarkers for each. While glucose (Glu) has been a well-recognized biomarker for diabetes, neurochemicals such as dopamine (DA) has been recognized as effective biomarker related to several neurodegenerative diseases such as post-traumatic stress disorder (PTSD), Parkinson's and chronic depression. Accordingly, these common diseases such as type II diabetes, Parkinson's, schizophrenia, and Alzheimer's can now be detected based on the levels of biomarkers, such as glucose, and dopamine, respectively.

Glucose is a vital biomolecule present in the body which helps in production of energy molecule adenosine triphosphate (ATP) through physiological processes. Typically, glucose is accumulated in the body from external sources including diet which is dependent on individual's habit and lifestyle. While considered an essential biomolecule, high levels of glucose can lead to several metabolic disorders such as diabetes mellitus as well as catastrophic failure including death. Currently glucose is detected by its presence in the bloodstream through the

use of enzymatic glucose sensors that rely on glucose-oxidase to estimate glucose concentration through indirect oxidation. Although amount of glucose present in blood is maximum, other physiological fluids such as urine [1], sweat [2], saliva [3], tears [4], and exhaled air can also be ideally used if the sensitivity of the device can be increased to be compatible with the low levels of glucose present in these other body fluids. Although enzyme-based glucose sensing strips are readily available to the consumers, there are several disadvantages for these sensors, including: non-reusability, instability due to rapid enzyme degradation, low sensitivity, as well as cost associated with enzyme isolation and stabilization. Non-enzymatic sensors that work on the principle of direct detection method can overcome some of these drawbacks. With good thermal and chemical stability, simple fabrication process, low costs, and good reproducibility, non-enzymatic sensors are more conducive to technological improvements and large-scale production [5, 6]. In that respect, electrochemical glucose sensors that can detect glucose through direct electro-oxidation has been at the center of attraction for the last few years. Recent efforts have led to breakthroughs in the development of non-enzymatic glucose sensors based on earth-abundant transition metal chalcogenides (TMCs) [7–9], transition metal phosphides (TMPs) [10, 11], transition metal

nitrides (TMNs) [12, 13], transition metal oxides [14, 15], transition metal hydroxides [16, 17], transition metal phosphates [18, 19] etc.

Dopamine (DA) is an organic chemical in the family of catecholamine and phenethylamine that is involved in neurotransmission and has been known to be responsible for several neurodegenerative disorders including Parkinson's disease and onset/progression of post-traumatic stress disorder (PTSD) [20, 21]. Current techniques for dopamine detection relies on analytical methods like colorimetry, fluorescence, and liquid chromatography [22–24]. These analytical techniques are time consuming and includes costly and specialized equipment in a laboratory setup. For dopamine, developing a method for continuous detection is also required since it has been proposed from several studies that the fluctuating dopamine concentration characteristic of an individual can be indicative of development of PTSD and related disorders. The common analytical techniques are not readily integrable into the continuous monitoring/detecting strips. However, since chemical composition of DA contains phenolic –OH groups, it can be electrochemically oxidized [25]. Electrochemical oxidation of dopamine can proceed through one or two electron pathways producing semi-quinone or quinone forms (Fig. 1). Hence, direct electro-oxidation of dopamine can be conceptually used for measuring levels of DA in various analytes [26]. Several electrochemical methods for detection of dopamine has been reported over the last few years [27–30]. Electrochemical methods are generally simple techniques, sensitive, and selective to specific analyte depending on their chemical composition, making them more efficient among all the

available approaches. In addition, direct electrochemical sensing also provides opportunity for point-of-care (POC) testing that has the potential to improve management of infectious diseases, especially in resource-limited settings where health care infrastructure is weak, and access to quality and timely medical care is a challenge. Direct electrochemical detection has several other advantages including rapid sampling rates, possibility of developing a flexible wearable sensor, and high biocompatibility of the electrode material [29, 31].

Both dopamine and glucose can be described as molecules with –OH functional groups, where oxidation leads to conversion of these –OH functional groups to ketonic (=O) groups and formation of dopamine-quinone or gluconolactone, respectively as shown schematically in Fig. 1. These electrochemical sensing methods typically use electrocatalyst-modified electrodes, where the role of electrocatalyst is to aid in oxidation of these biomolecules and enhance charge transfer between electrode to analyte (dopamine/glucose). In some cases, the analyte (dopamine/glucose) can attach to the surface of the electrocatalyst which facilitates charge transfer [9, 30]. Hence the chemical composition of the electrocatalyst plays an intriguing role in defining efficiency and selectivity of such sensors. Recently, transition metal dichalcogenide materials have attracted great attention as electrocatalysts in various electrochemical conversion reactions including photocatalysis [32], supercapacitor [33], oxygen reduction [34, 35], CO<sub>2</sub> reduction [36, 37], and water splitting [38, 39]. Several transition metal chalcogenides have been also used for dopamine as well as glucose sensing including nickel telluride, (Ni<sub>3</sub>Te<sub>2</sub>) [7], bismuth selenide, (Bi<sub>2</sub>Se<sub>3</sub>) [40], tin selenide, (SnSe) [41] etc.

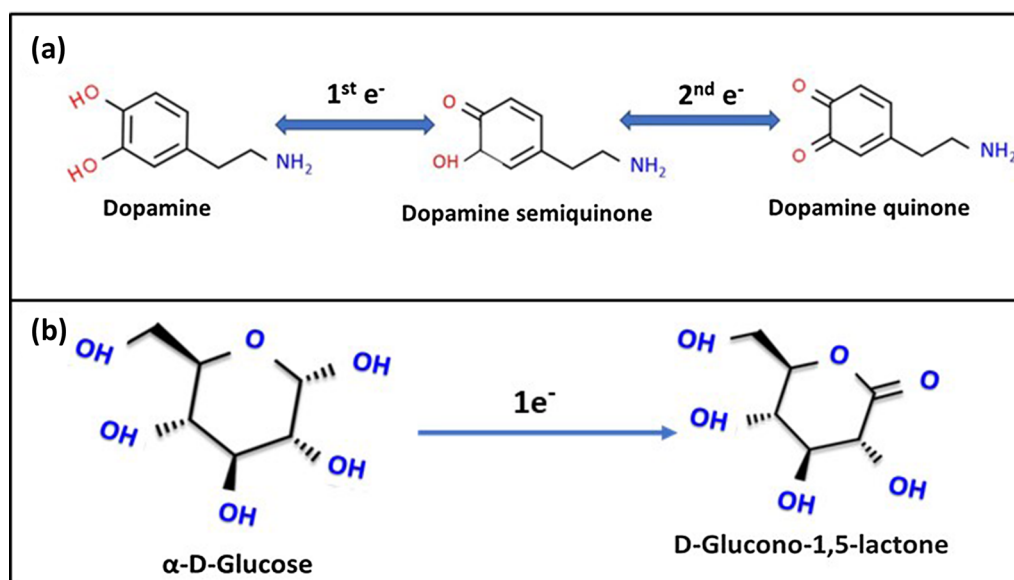


**Figure 1:** Scheme of (a) dopamine electro-oxidation and (b) glucose electro-oxidation on Cu<sub>2</sub>Se electrode.

Numerous materials have been investigated for glucose and dopamine sensor applications, with particular emphasis on gold due to its biocompatibility, high stability, and conductivity [42–45]. The high cost of gold, however, makes biomolecules sensing applications economically prohibitive. Therefore TMCs has become a promising alternative candidate for different non-enzymatic biosensors. The transition metal chalcogenides are characterized by their unique electronic properties and tunable electrochemical behavior which leads to possibilities of faster charge transfer kinetics. The availability of partially filled d-orbitals makes it possible for the transition metal chalcogenides (TMCs) to adopt diverse structures and compositions, with varying stoichiometries. Copper selenide is one of the metal chalcogenides that has gained considerable attention in recent years due to interesting electrocatalytic property [30, 38]. Copper selenide has various stoichiometric and non-stoichiometric compositions including CuSe, Cu<sub>2</sub>Se, Cu<sub>3</sub>Se<sub>2</sub>, Cu<sub>7</sub>Se<sub>4</sub>, Cu<sub>5</sub>Se<sub>4</sub>, Cu<sub>2</sub>Se, Cu<sub>2-x</sub>Se. These different compositions of copper selenide vary in their electronic properties, thermal stability, and bandgap [46–49]. In this article we have explored multifunctional electrocatalytic activity of Cu<sub>2</sub>Se for selective oxidation of glucose and dopamine. The Cu<sub>2</sub>Se was synthesized as nanostructured powder through one-pot hydrothermal technique. The Cu<sub>2</sub>Se-modified electrodes showed high sensitivity for detection of glucose (15.341 mA mM<sup>-1</sup> cm<sup>-2</sup>) and dopamine (12.43 μA μM<sup>-1</sup> cm<sup>-2</sup>) at different applied potentials of 0.35 and 0.2 V vs Ag|AgCl, respectively. The sensitivity obtained from dopamine detection is among the highest reported for non-enzymatic dopamine sensors. Interestingly, it was observed that Cu<sub>2</sub>Se modified electrode shows high selectivity for dopamine and glucose even in the presence of other interferents (e.g. ascorbic acid, uric acid, potassium chloride, sodium chloride, lactose, sucrose etc.) commonly found in physiological fluids. The sensor also shows high selectivity for detecting only dopamine and/or glucose from a mixture of the two analytes depending on the applied potential.

## Results and discussion

The as-synthesized Cu<sub>2</sub>Se was characterized using various techniques to determine its structural and morphological composition. Figure 2a shows the crystalline PXRD pattern of the hydrothermally synthesized product, which is well matched with the Cu<sub>2</sub>Se standard diffraction pattern (PDF No. 00–006–0680) indicating that the product was pure copper selenide. The strong and sharp diffraction peaks suggest that the as-synthesized compound has high degree of crystallinity. The typical field emission SEM (FESEM) image in Fig. 2b clearly shows a large quantity of randomly oriented granular nanoparticles with sizes in range of 60–80 nm. Such nanostructured geometry can be very beneficial for electrocatalytic activity since it enhances contact area between electrocatalyst and analyte.

The valence state of the constituent elements and the chemical composition of the catalyst were further investigated by XPS. Figure 2c shows the XPS peaks that can be attributed to Cu 2p<sub>3/2</sub>, Cu 2p<sub>1/2</sub> while the inset shows XPS signals for Se 3d<sub>5/2</sub>, and Se 3d<sub>3/2</sub>. The deconvoluted Cu 2p spectra shows peaks at 932.4 and 952.6 eV corresponding to Cu<sup>1+</sup> and 934.4 and 954.7 eV for Cu<sup>2+</sup> indicating presence of mixed oxidation states for Cu. Presence of such mixed oxidation states in Cu<sub>2</sub>Se has been reported previously [38, 50]. The Se XPS spectra on the other hand, shows peaks at 55.4 eV (Se 3d<sub>3/2</sub>) and 54.1 eV (Se 3d<sub>5/2</sub>) corresponding to the presence of Se [2, 38, 51].

### Electrochemical oxidation of dopamine

Different techniques of voltammetry are extremely useful in the analysis of various biological and chemical substances. Among these, square wave voltammetry (SWV) was chosen for the determination of DA in this research project, as it is the most advanced and sophisticated technique of pulse voltammetry. Dopamine detection was carried out in 0.1 M PBS (pH 7.0) electrolyte containing a known concentration of DA (1–640 μM). The electrochemical measurements were performed with SWV in the potential range from –0.1 to 0.5 V. First, the SWV

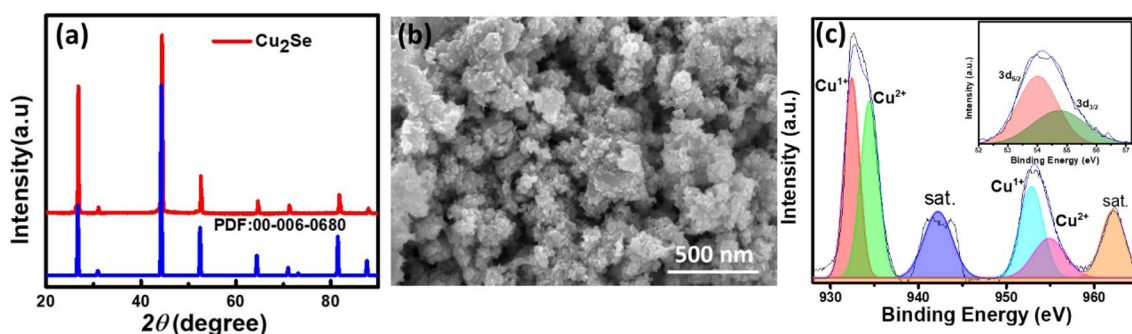


**Figure 2:** (a) PXRD pattern and (b) SEM image of hydrothermally synthesized Cu<sub>2</sub>Se. (c) XPS spectra of Cu<sub>2</sub>Se showing Cu 2p peaks while inset shows Se 3d peak.

parameters were optimized for improving this DA measuring system. The effects of frequency change on peak current was studied, showing that frequencies up to 50 Hz result in an increase in peak current. However, at higher frequencies the current decreases considerably. Therefore, the frequency of 50 Hz was used as our optimum frequency value. Also, an increase in peak current was observed by increasing pulse heights up to 40 mV. For SWV, higher pulse heights (> 40 mV) cause broadening of the spectra and decrease the intensity of the analyte peak current. Figure 3a shows the SWV curves for different concentration of DA and it can be observed from the curves that the oxidation potential of DA was at 0.2 V vs Ag/AgCl. A calibration curve was constructed by plotting the anodic peak current as a function of DA concentration. The calibration plot shows two linear regions, 1–30  $\mu\text{M}$  and 100–640  $\mu\text{M}$  as shown in Fig. 3b and Figure S1, respectively.

Cyclic voltammetry was also used to investigate electrochemical oxidation of dopamine in a 0.1 M PBS electrolyte solution at a scan rate of 10 mV/s. (Fig. 4). As shown in Fig. 4a, the  $\text{Cu}_2\text{Se}$ -modified electrode exhibits no obvious oxidation current

across the potential range, when measured in a PBS solution without DA. However, after adding 10  $\mu\text{M}$  DA, there was a significant increase in the oxidation peak at 0.2 V indicating oxidation of dopamine. Chronoamperometric studies were utilized to investigate dopamine oxidation on  $\text{Cu}_2\text{Se}$ -modified electrode further, where different concentrations of dopamine were added to the electrolyte while maintaining a constant applied potential (0.2 V) and increase in oxidation current was measured. In CV and SWV measurements, the oxidation peak at 0.2 V increased remarkably with the increase in DA concentration. Hence, 0.2 V was used as a working electrode potential for all chronoamperometric experiments. The representative chronoamperometric current (I) vs time (t) curve showing  $\text{Cu}_2\text{Se}$  response to successive addition of different DA concentrations is shown in Fig. 4b. The chronoamperometry plot further show that the increase in oxidation current is proportional to the increase in DA concentration. A calibration plot was constructed by plotting the anodic peak current as a function of dopamine concentration as shown in Fig. 4c. The calibration plot shows a linear region in the low concentration range. Sensitivity of the electrode could

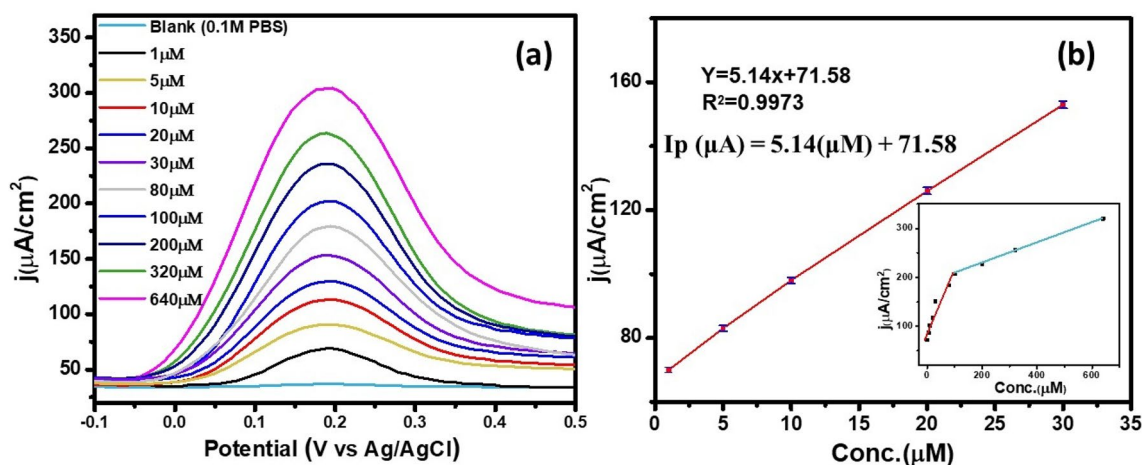


**Figure 3:** (a) SWV plots of  $\text{Cu}_2\text{Se}$  in 0.1 M PBS buffer in the presence of increasing concentrations of DA. (b) Corresponding calibration curve showing linear fit in the concentration range of 1–30  $\mu\text{M}$  [ $I_p$  = anodic peak current]. Inset shows peak current vs concentration of DA at low and high DA concentration.

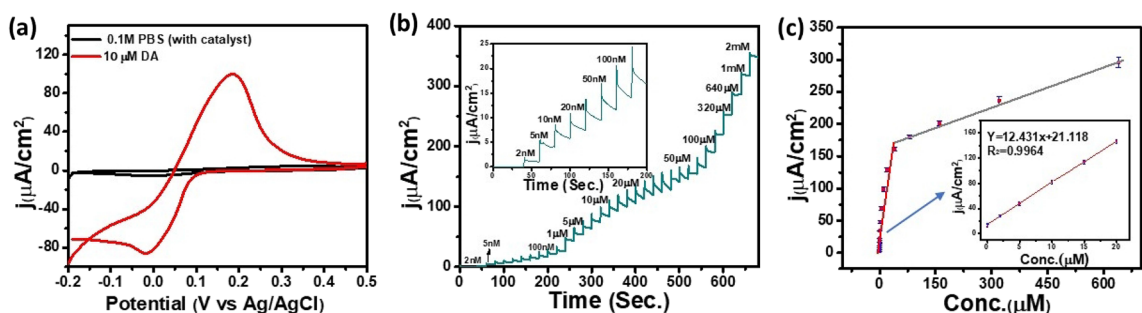


**Figure 4:** (a) CV of  $\text{Cu}_2\text{Se}$  catalyst with 10  $\mu\text{M}$  of DA and without DA. (b) Chronoamperometric measurements of  $\text{Cu}_2\text{Se}$  catalyst at 0.2V potential vs Ag/AgCl. (c) Peak current vs concentration of DA at low and high DA concentration. Inset shows the linear range from 2 nM to 30  $\mu\text{M}$ .

be estimated as  $12.43 \mu\text{A } \mu\text{M}^{-1} \text{cm}^{-2}$  from slope of the linear region in the low concentration range of 2 nM to 30  $\mu\text{M}$  (inset of Fig. 4c). The limit of detection (LOD) of the DA sensor could be calculated from the equation:

$$\text{LOD} = \frac{3S}{m} \quad (1)$$

Here  $S$  is the standard deviation obtained from the blank signals (measured in electrolyte devoid of added DA), and  $m$  is the slope value extracted from the calibration plot. Using this equation LOD is estimated to be 84 nM. This low value of LOD and high sensitivity for DA detection makes this catalyst most efficient. The second linear region from the higher concentration range of 80  $\mu\text{M}$  to 640  $\mu\text{M}$  showed the sensitivity of  $1.34 \mu\text{A } \mu\text{M}^{-1} \text{cm}^{-2}$  as shown in Figure S2.

### Electrochemical oxidation of glucose

Electrochemical oxidation of glucose on  $\text{Cu}_2\text{Se}$  modified carbon cloth electrodes was investigated by cyclic voltammetry (CV) at a scan rate of  $10 \text{ mV s}^{-1}$  in 0.1 M NaOH electrolyte. In Fig. 5a, the glucose oxidation potential of the  $\text{Cu}_2\text{Se}$ -modified electrode was initially measured by collecting CV plots in absence and presence of glucose in the electrolyte. It was observed that while there was no oxidation current in absence of glucose, the oxidation current increased with increasing glucose concentration from 0.25 mM to 1 mM and the oxidation potential was obtained at 0.35 V (onset potential). Hence, for further chronoamperometry measurements, applied potential was chosen to be 0.35 V (vs. Ag/AgCl). Figure 5b shows chronoamperometric measurements of the  $\text{Cu}_2\text{Se}$ -modified working electrode as a function of successive addition of different concentration of glucose in the range of 0.25  $\mu\text{M}$  – 8 mM. The effect of addition of low concentration of glucose has been shown much clearly in inset of Fig. 5b which shows the chronoamperometric curve when concentrations of glucose are in the range of 0.25  $\mu\text{M}^{-1} \mu\text{M}$ . Figure 5c shows the calibration curve constructed by plotting

anodic peak current vs glucose concentration from the chronoamperometric experiment. It was observed that there were two linear ranges in the calibration plot, 0.25  $\mu\text{M}$ -40  $\mu\text{M}$  and 80  $\mu\text{M}$  to 8 mM. The sensitivity of the sensor was estimated from the linear region in the lower concentration range which showed a value of  $15.341 \text{ mA mM}^{-1} \text{cm}^{-2}$ . The LOD was calculated to be 0.26  $\mu\text{M}$ . Figure S3 shows the calibration curve in higher concentration range (80  $\mu\text{M}$  to 8 mM) from which sensitivity was also estimated as  $1.89 \text{ mA mM}^{-1} \text{cm}^{-2}$ . Such high sensitivity suggests high efficiency of  $\text{Cu}_2\text{Se}$  for non-enzymatic glucose detection.

### Advantages of chalcogenide matrices for electrocatalysis

Transition metal chalcogenides, as has been mentioned before, provides significant enhancements for electrochemical reactions on its surface owing to several factors. Firstly, the lower electronegativity of the chalcogenide anions leads to increased covalency in the lattice which in turn facilitates charge transfer across the chalcogenide matrix by reducing bandgap as well as increasing electronic conductivity. Secondly, the lower electronegativity of chalcogenide anion increases electron density around the catalytically active transition metal center, which in turn, tunes the electrochemical activation steps. As shown in Fig. 1, both dopamine and glucose oxidation converts the -OH functional groups to ketonic (=O) functional group. Typically, these analyte (dopamine and glucose) molecules anchor on the catalytically active site through attachment of the -OH functional group to the transition metal site through coordination bond, leading to catalyst activation. Such -OH adsorption on the transition metal site is facilitated by local site oxidation of the active site. Previously it had been observed that local site oxidation of these transition metal chalcogenide-based electrocatalysts could be enhanced as a function of decreasing anion electronegativity leading to lower catalyst activation potential for selenides and tellurides [52, 53]. Hence, it can be expected that for this copper

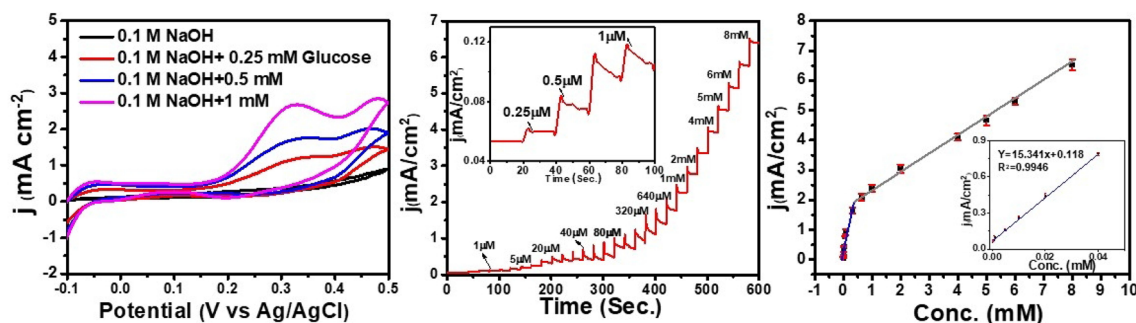


**Figure 5:** (a) CV plots of  $\text{Cu}_2\text{Se}$  catalyst with 0.25 mM, 0.5 mM and 1 mM of glucose and without glucose. Chronoamperometric measurements of  $\text{Cu}_2\text{Se}$  catalyst at 0.35 V potential vs Ag/AgCl. Peak current vs concentration of glucose at low and high glucose concentration. Inset shows the linear range from 0.25 to 1  $\mu\text{M}$ .

selenide-based electrocatalysts, the analyte adsorption on the active site can occur at lower applied potential owing to the facile local site oxidation of Cu [9, 30]. The enhanced electron density around catalytically active site further leads to increased charge transfer and higher oxidation current, resulting in higher sensitivity for dopamine and glucose sensing.

### Effect of interference

Another significant factor and challenge for electrochemical sensors in practical applications is the selectivity for DA and/or glucose detection, in the presence of other interferents commonly present in bodily fluids. Hence, the interference study was performed by investigating efficacy of dopamine detection in the presence of different interferents such as ascorbic acid (AA), glucose (GLU), uric acid (UA), KCl, and NaCl. A chronoamperometric experiment was performed where the Cu<sub>2</sub>Se-modified electrode was maintained at a constant applied potential of +0.2 V vs Ag|AgCl in 0.1 M PBS electrolyte, while known concentrations (0.1 mM) of DA and other interfering compounds were added successively to the same electrolyte, as shown in Fig. 6a. Sharp current responses were observed for the additions of 0.1 mM DA, while addition of other interferents did not show any significant current responses. Furthermore, same concentration of DA was added at the end of chronoamperometry experiment to check the reproducibility of electrode after exposing through other chemical compounds, which showed same current response as the initial DA addition indicating high reproducibility of the electrode. Hence it was confirmed that the Cu<sub>2</sub>Se catalyst showed negligible interference from other analytes commonly found in physiological fluids and was selective towards only DA oxidation at 0.2 V vs Ag|AgCl.

Selectivity for glucose sensing at 0.35 V vs Ag|AgCl in presence of other interferents was also investigated in a similar chronoamperometric measurement performed at 0.35 V vs Ag|AgCl in 0.1 M NaOH where the glucose and other interfering compounds were added successively to the same electrolyte. In order to confirm the selectivity of the glucose, different concentration of interferents such as dopamine (DA), ascorbic acid (AA), Uric Acid (UA), potassium chloride (KCl), sodium chloride (NaCl), lactose (LA) and sucrose (SU) were injected along with the glucose solution (0.1 mM). Figure 6b shows the chronoamperometry plot where it can be seen that only addition of glucose produces an increase in the oxidation current at an applied potential of 0.35 V, while the other interferents do not show any change. Hence it was confirmed that Cu<sub>2</sub>Se was also selective towards glucose oxidation at 0.35 V vs Ag|AgCl.

The reproducibility of the Cu<sub>2</sub>Se electrode toward dopamine and glucose oxidation was also investigated by adding 0.1 mM of glucose and DA in 0.1 M NaOH and 0.1 M PBS, respectively under constant stirring. Chronoamperometry tests as shown in Fig. 7a and b investigated the long-term stability of the electrode for DA and glucose detection, respectively. In Fig. 7a, as 0.1 mM of glucose was added to the electrolyte at a constant applied potential of +0.35 V vs Ag|AgCl, there was sharp increase in oxidation current which decreases gradually over time as the added glucose in the electrolyte was oxidized. Then after 10,000 s, same amount of fresh glucose solution was added to the solution, which immediately showed almost same increase in oxidation current. Such study confirmed reproducibility and reusability of the electrode for glucose oxidation. Similarly, long-term stability and reproducibility for DA oxidation was checked from chronoamperometry studies at an applied potential of +0.2 V vs Ag|AgCl (Fig. 7b). As it can be observed from Fig. 7b, successive additions of dopamine

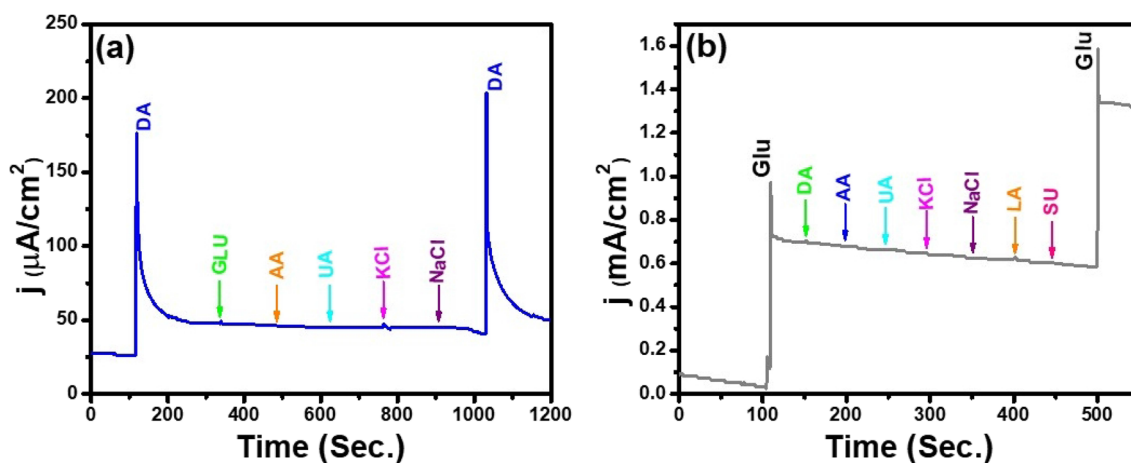


**Figure 6:** (a) The chronoamperometric response of DA oxidation on Cu<sub>2</sub>Se electrode in 0.1 M PBS electrolyte with successive additions of 0.1 mM dopamine and other common interferents (AA (0.5 mM), GLU (0.5 mM), UA (0.5 mM), KCl (0.5 mM) and NaCl (0.5 mM)). (b) The chronoamperometric response of glucose oxidation on the Cu<sub>2</sub>Se electrode in 0.1 M NaOH electrolyte with the successive additions of 0.1 mM glucose and other common interferents DA (0.5 mM), AA (0.5 mM), UA(0.5 mM), KCl (0.5 mM), NaCl (0.5 mM), LA(0.1 mM) and SU (0.1 mM)).

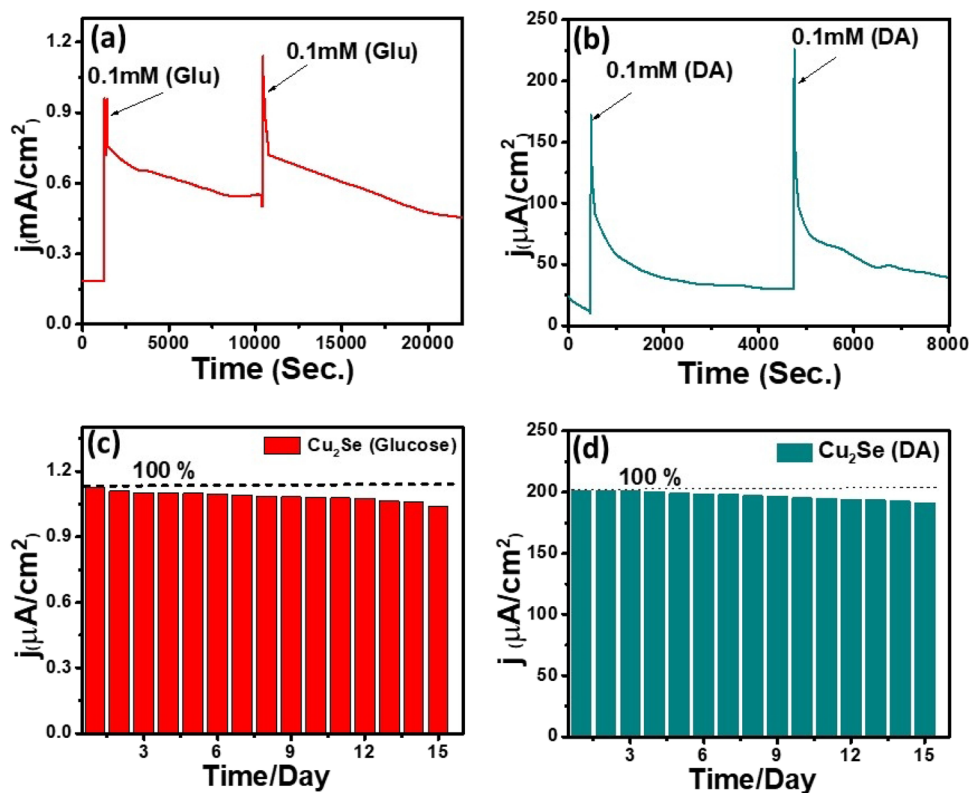


**Figure 7:** (a) The chronoamperometric response at applied potential of 0.35 V in 0.1 M NaOH for long-term stability and reproducibility of glucose sensor. (b) The chronoamperometric response at applied potential of 0.20 V in 0.1 M PBS for long-term stability and reproducibility of DA sensor. (c) Stability of the glucose and (d) DA sensors for 15 days showing reproducible current signal upon daily addition of 0.1 mM glucose and 0.1 mM DA, respectively.

(0.1 mM) after a long-time gap retains almost same peak current, indicating reproducibility of the electrode. These chronoamperometry studies also illustrates long-term functional stability of this Cu<sub>2</sub>Se-modified electrode towards DA and glucose sensing. The long-term stability of the glucose and dopamine sensor was also tested by measuring glucose and dopamine oxidation currents repeatably from standard solution with the same electrode stored under ambient condition for a period of 15 days. After 15 days, the glucose sensor reached almost ~91% of its original response and DA sensor retained 94.5% current response indicating excellent stability of Cu<sub>2</sub>Se electrode for both dopamine and glucose sensing. The compositional stability of the Cu<sub>2</sub>Se-modified electrodes after dopamine and glucose sensing activity as analyzed through XPS. The XPS spectra of Cu<sub>2</sub>Se after electrochemical activity showed almost no change compared to as-synthesized Cu<sub>2</sub>Se (Figure S4) confirming that the electrode was indeed stable under operational conditions for DA and GLU sensing.

Further, the excellent bifunctional electrocatalytic activity of Cu<sub>2</sub>Se nanostructure towards oxidation of two separate biomolecules was also investigated by a CV experiment (Fig. 8a) conducted in 0.1 M PBS (pH 7.0) electrolyte containing a mixture of DA and glucose with same concentration of each (10 μM). Firstly, a CV experiment was performed measuring the

current with Cu<sub>2</sub>Se-modified electrode in 0.1 M PBS electrolyte to check for possible oxidation peaks from the electrode and/or electrolyte itself. As shown in Fig. 8a, no current response was detected in PBS in absence of dopamine or glucose in the potential range of -0.2 to 0.55 V vs Ag|AgCl. On the contrary, when equal amounts of DA and glucose were mixed in the 0.1 M PBS solution, two well-defined oxidation peaks with large peak separations were observed in the CV experiment, corresponding to oxidation of DA (~0.2 V) and glucose (~0.35 V). 10 μM of DA solution and 10 μM of glucose solution added to 0.1 M PBS separately showed similar oxidation peaks as has been depicted with dashed lines in the CV plot shown in Fig. 8a, confirming that there was minimal shift of the individual oxidation peaks in mixture of dopamine and glucose. Specifically, dopamine oxidation peak showed a slight shift of ~50 mV in the mixture compared to dopamine by itself. Such slight shift can be possibly explained by the change in ionic concentration around the active site in presence of another analyte (glucose) [54]. Nevertheless, this CV experiment showing significant separation between oxidation peak positions further confirmed that Cu<sub>2</sub>Se nanostructure can indeed be used to fabricate an electrochemical sensor for simultaneous detection of dopamine and glucose in a mixture with high selectivity for each. The analyte selectivity



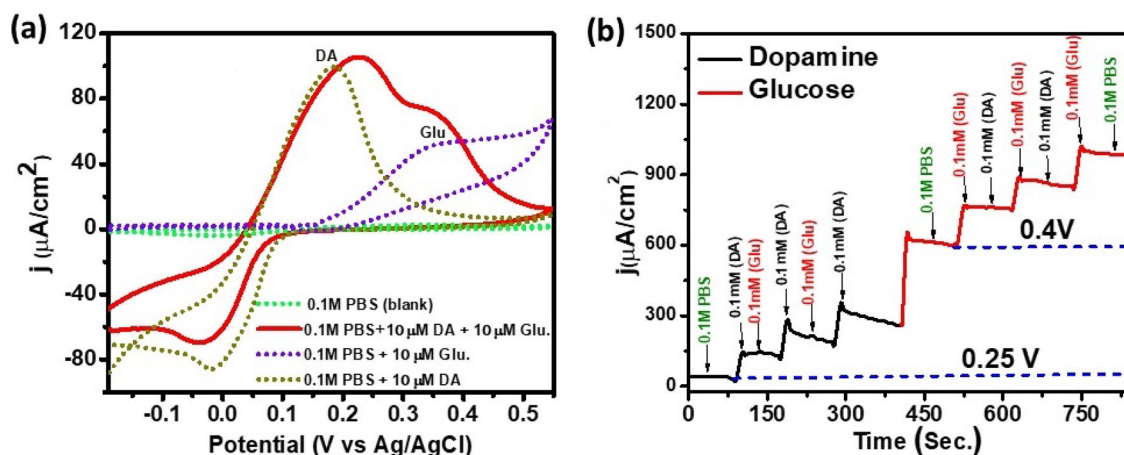


**Figure 8:** (a) CV response of  $\text{Cu}_2\text{Se}$ -modified electrode with the addition of 10  $\mu\text{M}$  DA and 10  $\mu\text{M}$  of glucose in PBS (pH  $\sim$  7) solution. (b) Multistep-chronoamperometry by successive addition of 0.1 mM DA and 0.1 mM glucose as well 0.1 M of PBS solution at 0.25 V and 0.4 V of applied potential illustrating analyte selectivity at different applied potentials.

in this case depends on the applied potential for measurement. Such bifunctional activity was also investigated from multistep chronoamperometry experiment where the current response as a function of successive glucose and dopamine additions to the same electrolyte (0.1 M PBS) was investigated at two applied potentials (0.25 V and 0.4 V vs Ag|AgCl) as shown in Fig. 8b. It was observed that at 0.25 V the  $\text{Cu}_2\text{Se}$ -modified electrode showed oxidation current only upon addition of dopamine (0.1 mM) to the electrolyte, while addition of PBS (100  $\mu\text{L}$  of 0.1 M solution) as well as glucose (0.1 mM) did not result in any increase of the oxidation current. On the other hand, at applied potential of 0.4 V, addition of only glucose produced significant change in oxidation current, while dopamine and PBS addition failed to produce any current response. 100  $\mu\text{L}$  of 0.1 M PBS solution was added at each potential step in the beginning as control experiment to check for any instantaneous current response resulting from electrolyte perturbation. As can be seen from Fig. 8b, instantaneous current response from such perturbations were negligible. This chronoamperometry experiment further confirmed that high degree of sensitivity and selectivity can be achieved with  $\text{Cu}_2\text{Se}$ -modified electrode for individual or simultaneous detection of these biomolecules, glucose and dopamine.

### Determination of glucose in human blood samples

The non-enzymatic glucose sensor was tested by measurement of glucose in human blood samples using a standard process [55, 56] and compared with reading from commercially available enzymatic glucometer (ReliOn). The chronoamperometry studies were performed to detect glucose levels in whole blood samples at applied potential of 0.35 V (vs Ag|AgCl). In this experiment, 1 mM of standard glucose solution (100  $\mu\text{L}$ )

was added twice to 0.1 M NaOH electrolyte and then 100  $\mu\text{L}$  of blood sample injected to the electrolyte. 1 mM of standard glucose solution was injected again two times to record the current response from the electrode. A calibration curve was constructed by plotting the current response as a function of standard glucose additions, which showed a linear response as expected. Figure 9 shows such linear plot of the glucose sensor for two different experiments. Concentration of glucose in blood sample was detected by mapping the current response obtained from blood sample in this calibration plot and estimating the corresponding concentration. The standard deviation was obtained by performing each addition experiment 3 times. Table S1 shows the glucose concentration values obtained from glucometer as well as from the  $\text{Cu}_2\text{Se}$ -based electrode for glucose sensor. It was observed that the glucose level detected from this sensor was very close to that obtained from glucometer further confirming reliability of these readings.

### Determination of dopamine level in human blood samples

The fabricated  $\text{Cu}_2\text{Se}$ -based electrode was also used to determine dopamine concentration in human blood samples without pre-treatment. The chronoamperometry experiment was performed in a similar way as explained above using an applied potential of 0.2 V (vs Ag|AgCl). A standard dopamine solution of known concentration (5 nM) was added 2 times before and after addition of blood sample to 0.1 M PBS solution. A calibration plot was constructed by plotting the current response as a function of dopamine concentration of the standard additions, which showed a linear response as shown in Fig. 10. The dopamine level in added blood samples was estimated by mapping the corresponding current density in this calibration plot as shown in

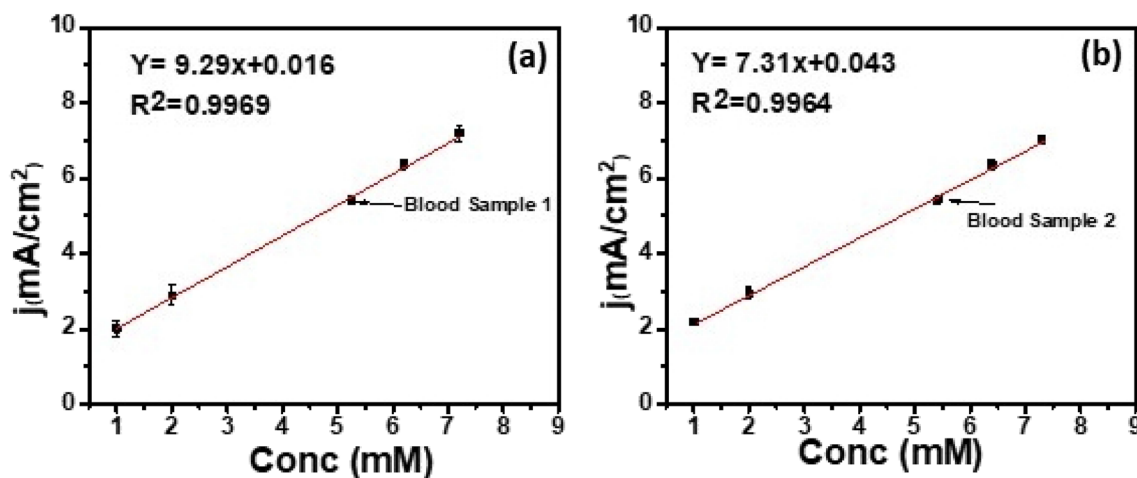


**Figure 9:** Glucose measurement of collected in (a) Blood sample 1 (b) Blood sample 2. Plot represents the fitted linear plot of current response vs glucose concentration.

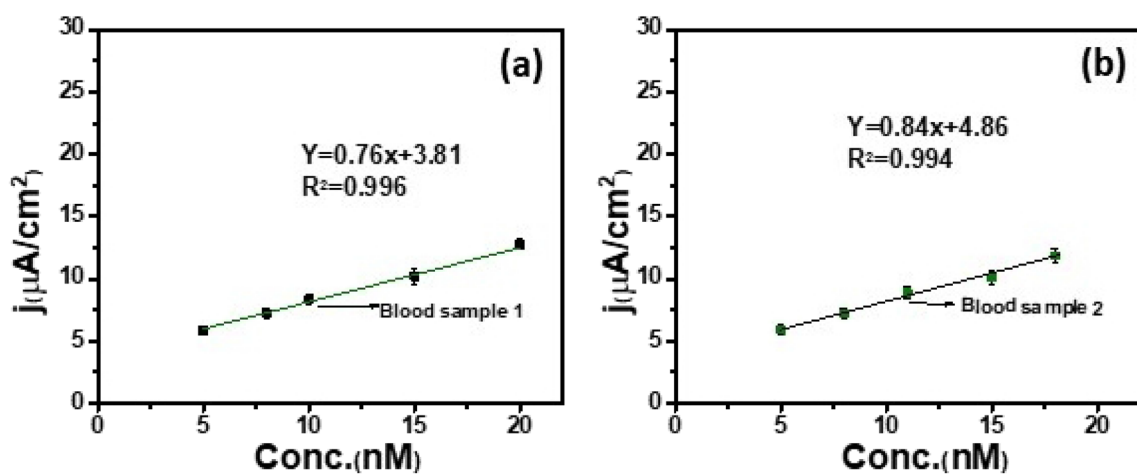


**Figure 10:** Measurement of dopamine amount in (a) Blood sample 1, and (b) Blood sample 2. Plot represents the fitted linear plot of current response vs dopamine concentration.

the figure. The DA concentration in 2 different blood samples were determined as 9 nM and 11.5 nM which is similar to typical dopamine concentration detected in physiological samples.

### Conclusion

Hydrothermally synthesized copper selenide has been identified as highly efficient bifunctional electrochemical sensor for non-enzymatic detection of biomolecules glucose and dopamine which are considered biomarkers for various diseases. This Cu<sub>2</sub>Se modified electrode can oxidize dopamine and glucose at low applied potential (0.2 V and 0.35 V vs Ag|AgCl, respectively) with high sensitivity for detection. A comparison of this Cu<sub>2</sub>Se-based sensor with other Cu-based sensors for dopamine and glucose detection (Tables S2 and S3 in supporting information) showed that the bifunctional Cu<sub>2</sub>Se-based sensor reported

in this article shows one of the highest sensitivities and lowest applied potential for both glucose and dopamine sensing. Such enhancement of sensor performance can be attributed to the increased covalency around the catalytically active center that facilitates catalyst activation step as well as charge transfer across the matrix. This copper selenide-based sensor also exhibits high selectivity towards glucose and dopamine detection in presence of other interferences. It also exhibits high specificity for dopamine and glucose detection dependent on the applied potential where only one analyte is detected at a certain applied potential. These sensors also showed high reproducibility where the same sensing strip could be reused repeatedly for over couple of weeks and produced similar reading for same concentration of glucose and/or dopamine in the analyte. Such high degree of reproducibility, selectivity and specificity along with high sensitivity makes this bifunctional sensor attractive for integrating into

continuous monitoring devices that can ideally use other body fluids to sense these important biomarkers and offer proper point-of-care diagnosis and preventative care.

## Experimental

All the reagents were of analytical grade and were used as received. Dextrose, dopamine (DA), ascorbic acid, sodium chloride, potassium chloride, uric acid, sucrose and lactose were obtained from Fisher Scientific, and fructose from Sigma-Aldrich. Copper oxide ( $\text{Cu}_2\text{O}$ ), Selenium (Se) and hydrazine hydrate ( $\text{N}_2\text{H}_4\cdot\text{H}_2\text{O}$ ) were purchased from Acros Organics.

Synthesis of  $\text{Cu}_2\text{Se}$ : Copper selenide was synthesized by an improved hydrothermal process based on the synthesis method reported in our previous publication [38]. In a typical synthesis method, equal molar ratio of copper oxide ( $\text{Cu}_2\text{O}$ ) and Selenium (Se) powder was taken. The original molar ratio between  $\text{Cu}_2\text{O}$  and Se was selected to be 1:1. Firstly,  $\text{Cu}_2\text{O}$  (0.001 M) was put into a Teflon-liner of 23 mL capacity acid digestion bomb and dissolved in 8 ml of deionized water. After mixing for 20 min under vigorous stirring, Se (0.001 M) was added to the mixture. Finally,  $\text{N}_2\text{H}_4\cdot\text{H}_2\text{O}$  (3 ml) were added to the mixture, and the mixture was stirred continuously for another 20 min. The final mixture was sealed and heated at 185 °C for 24 h in Teflon-lined stainless-steel autoclave. The autoclave was then allowed to cool down naturally. The final product was then centrifuged and washed several times with a mixture of ethanol and deionized water. Finally, the product obtained was dried at 60 °C in a vacuum oven.

## Electrode preparation

To analyze the activity of hydrothermally synthesized  $\text{Cu}_2\text{Se}$ , a homogeneous catalyst ink was prepared by adding 4 mg of catalyst powder in 300  $\mu\text{L}$  of ethanol mixed with Nafion (0.8  $\mu\text{L}$  5 wt %). This mixture was ultra-sonicated for about 1 h to prepare a homogeneous ink. 40  $\mu\text{L}$  of the ink was drop casted onto carbon cloth (geometric area of 0.08  $\text{cm}^2$ ), leading to the catalyst loading  $\sim 0.53 \text{ mg}\cdot\text{cm}^{-2}$ .

## Characterization

Powder X-ray diffraction (PXRD) patterns were recorded using Philip X-Pert powder X-Ray diffractometer using Ni-filtered  $\text{Cu-K}\alpha$  radiation of 1.5406 Å, within the  $2\theta$  range between 20° and 90° with the step of 0.025°. The morphology of the as-synthesized sample was analyzed using the FEI Helios Nanolab 600 scanning electron microscope with an acceleration voltage of 10 kV and a working distance of 5 mm. In addition, X-ray Photoelectron Spectroscopy (XPS) was performed using a KRATOS AXIS 165 spectrometer with an Al X-ray source to analyze

the surface chemical composition. All XPS data were collected without sputtering to analyze the true surface chemistry. All electrochemical tests were performed using an IviumStat potentiostat. The electrochemical measurements were performed in three-electrode cell system with a graphite rod as the counter electrode,  $\text{Ag}|\text{AgCl}$  (KCl-saturated) as the reference electrode and carbon cloth as working electrode.

## Acknowledgments

The authors would like to acknowledge Materials Research Center for equipment usage.

## Data Availability

Data related to the manuscript content will be made available upon request.

## Declarations

**Conflict of interest** The authors declare that they have no conflict of interest.

## Supplementary Information

The online version contains supplementary material available at <https://doi.org/10.1557/s43578-021-00227-0>.

## References

1. X. Kang, Z. Mai, X. Zou, P. Cai, J. Mo, A novel glucose biosensor based on immobilization of glucose oxidase in chitosan on a glassy carbon electrode modified with gold-platinum alloy nanoparticles/multiwall carbon nanotubes. *Anal. Biochem.* **369**(1), 71 (2007)
2. E. Cho, M. Mohammadifar, S. Choi: A self-powered sensor patch for glucose monitoring in sweat, *2017 IEEE 30th International Conference on Micro Electro Mechanical Systems (MEMS)*, 366–369 (2017)
3. W. Zhang, Y. Du, M.L. Wang, On-chip highly sensitive saliva glucose sensing using multilayer films composed of single-walled carbon nanotubes, gold nanoparticles, and glucose oxidase. *Sens. Bio-Sensing Res.* **4**, 96 (2015)
4. S.H. Lee, Y.C. Cho, Y. Bin Choy, Noninvasive self-diagnostic device for tear collection and glucose measurement. *Sci. Rep.* **9**(1), 1 (2019)
5. G. Wang, X. He, L. Wang, A. Gu, Y. Huang, B. Fang, B. Geng, X. Zhang, Non-enzymatic electrochemical sensing of glucose. *Microchim. Acta* **180**(3–4), 161 (2013)
6. H. Zhu, L. Li, W. Zhou, Z. Shao, X. Chen, Advances in non-enzymatic glucose sensors based on metal oxides. *J. Mater. Chem. B* **4**(46), 7333 (2016)

7. B. Golrokh Amin, U. De Silva, J. Masud, M. Nath, Ultrasensitive and highly selective Ni<sub>3</sub>Te<sub>2</sub> as a nonenzymatic glucose sensor at extremely low working potential. *ACS Omega* **4**(6), 11152 (2019)
8. N. Vishnu, P. Sahatiya, C.Y. Kong, S. Badhulika, Large area, one step synthesis of NiSe<sub>2</sub> films on cellulose paper for glucose monitoring in bio-mimicking samples for clinical diagnostics. *Nanotechnology* **30**(35), 355502 (2019)
9. S. Umaphathi, H. Singh, J. Masud, M. Nath: Nanostructured copper selenide as an ultrasensitive and selective non - enzymatic glucose sensor. *Mater. Adv.* **2**(3), 927–932 (2021)
10. T. Chen, D. Liu, W. Lu, K. Wang, G. Du, A.M. Asiri, X. Sun, Three-dimensional Ni<sub>2</sub>P nanoarray: an efficient catalyst electrode for sensitive and selective nonenzymatic glucose sensing with high specificity. *Anal. Chem.* **88**(16), 7885 (2016)
11. Y. Liu, X. Cao, R. Kong, G. Du, A.M. Asiri, Q. Lu, X. Sun, Cobalt phosphide nanowire array as an effective electrocatalyst for non-enzymatic glucose sensing. *J. Mater. Chem. B* **5**(10), 1901 (2017)
12. J. Chen, H. Yin, J. Zhou, J. Gong, L. Wang, Y. Zheng, Q. Nie, Non-enzymatic glucose sensor based on nickel nitride decorated nitrogen doped carbon spheres (Ni<sub>3</sub>N/NCS) via facile one pot nitridation process. *J. Alloys Compd.* **797**, 922 (2019)
13. F. Xie, T. Liu, L. Xie, X. Sun, Y. Luo, Metallic nickel nitride nanosheet: an efficient catalyst electrode for sensitive and selective non-enzymatic glucose sensing. *Sens. Actuat. B Chem.* **255**, 2794 (2018)
14. V. Vinoth, T.D. Shergilin, A.M. Asiri, J.J. Wu, S. Anandan, Facile synthesis of copper oxide microflowers for nonenzymatic glucose sensor applications. *Mater. Sci. Semicond. Process.* **82**(March), 31 (2018)
15. S. Sedaghat, C.R. Piepenburg, A. Zareei, Z. Qi, S. Peana, H. Wang, R. Rahimi, Laser-induced mesoporous nickel oxide as a highly sensitive nonenzymatic glucose sensor. *ACS Appl. Nano Mater.* **3**(6), 5260 (2020)
16. P. Balasubramanian, S. BinHe, H.H. Deng, H.P. Peng, W. Chen, Defects engineered 2D ultrathin cobalt hydroxide nanosheets as highly efficient electrocatalyst for non-enzymatic electrochemical sensing of glucose and L-cysteine. *Sens. Actuat. B Chem.* **320**(1), 128374 (2020)
17. S. Moolayadukkam, S. Thomas, R.C. Sahoo, C.H. Lee, S.U. Lee, H.S.S.R. Matte, Role of transition metals in layered double hydroxides for differentiating the oxygen evolution and nonenzymatic glucose sensing. *ACS Appl. Mater. Interfaces* **12**(5), 6193 (2020)
18. S.S. Pujari, S.A. Kadam, Y.R. Ma, S.A. Khalate, P.K. Katkar, S.J. Marje, U.M. Patil, Highly sensitive hydrothermally prepared nickel phosphate electrocatalyst as non-enzymatic glucose sensing electrode. *J. Porous Mater.* **28**, 369–381 (2020)
19. X. Wang, M. Wang, S. Feng, D. He, P. Jiang, Controlled synthesis of flower-like cobalt phosphate microsheet arrays supported on Ni foam as a highly efficient 3D integrated anode for non-enzymatic glucose sensing. *Inorg. Chem. Front.* **7**(1), 108 (2019)
20. M.O. Klein, D.S. Battagello, A.R. Cardoso, D.N. Hauser, J.C. Bittencourt, R.G. Correa, Dopamine: functions, signaling, and association with neurological diseases. *Cell. Mol. Neurobiol.* **39**(1), 31 (2019)
21. F. Antonelli, A.P. Strafella, Behavioral disorders in Parkinson's disease: the role of dopamine. *Park. Relat. Disord.* **20**(SUPPL\_1), S10 (2014)
22. Z. Chen, C. Zhang, T. Zhou, H. Ma, Gold nanoparticle based colorimetric probe for dopamine detection based on the interaction between dopamine and melamine. *Microchim. Acta* **182**(5–6), 1003 (2015)
23. X. Chen, N. Zheng, S. Chen, Q. Ma, Fluorescence detection of dopamine based on nitrogen-doped graphene quantum dots and visible paper-based test strips. *Anal. Methods* **9**(15), 2246 (2017)
24. H.X. Zhao, H. Mu, Y.H. Bai, H. Yu, Y.M. Hu, A rapid method for the determination of dopamine in porcine muscle by pre-column derivatization and HPLC with fluorescence detection. *J. Pharm. Anal.* **1**(3), 208 (2011)
25. S. Schindler, T. Bechtold, Mechanistic insights into the electrochemical oxidation of dopamine by cyclic voltammetry. *J. Electroanal. Chem.* **836**(January), 94 (2019)
26. J.J. Van Dersarl, A. Mercanzini, P. Renaud, Integration of 2D and 3D thin film glassy carbon electrode arrays for electrochemical dopamine sensing in flexible neuroelectronic implants. *Adv. Funct. Mater.* **25**(1), 78 (2015)
27. K. Jackowska, P. Krysinski, New trends in the electrochemical sensing of dopamine. *Anal. Bioanal. Chem.* **405**(11), 3753 (2013)
28. J. Wang, H. Xu, S. Li, B. Yan, Y. Shi, C. Wang, Y. Du, Plasmonic and photo-electrochemical enhancements of the AuAg@Au/RGO-C<sub>3</sub>N<sub>4</sub> nanocomposite for the detection of da. *Analyst* **142**(24), 4852 (2017)
29. M. Mathew, S. Radhakrishnan, A. Vaidyanathan, B. Chakraborty, C.S. Rout, Flexible and wearable electrochemical biosensors based on two-dimensional materials: recent developments. *Anal. Bioanal. Chem.* **413**(3), 727 (2021)
30. S. Umaphathi, J. Masud, H. Coleman, M. Nath, Electrochemical sensor based on CuSe for determination of dopamine. *Microchim. Acta* **187**(8), 1–3 (2020)
31. F. Arduini, L. Micheli, D. Moscone, G. Palleschi, S. Piermarini, F. Ricci, G. Volpe, Electrochemical biosensors based on nanomodified screen-printed electrodes: Recent applications in clinical analysis. *TrAC - Trends Anal. Chem.* **79**, 114 (2016)
32. Y. Ji, M. Yang, H. Lin, T. Hou, L. Wang, Y. Li, S.T. Lee, Janus structures of transition metal dichalcogenides as the heterojunction photocatalysts for water splitting. *J. Phys. Chem. C* **122**(5), 3123 (2018)
33. B.G. Amin, J. Masud, M. Nath, Facile one-pot synthesis of NiCo<sub>2</sub>Se<sub>4</sub>-rGO on Ni foam for high performance hybrid supercapacitors. *RSC Adv.* **9**(65), 37939 (2019)

34. J. Masud, M. Nath,  $\text{Co}_7\text{Se}_8$  nanostructures as catalysts for oxygen reduction reaction with high methanol tolerance. *ACS Energy Lett.* **1**(1), 27 (2016)
35. S. Umaphathi, J. Masud, A.T. Swesi, M. Nath,  $\text{FeNi}_2\text{Se}_4$ -reduced graphene oxide nanocomposite: enhancing bifunctional electrocatalytic activity for oxygen evolution and reduction through synergistic effects. *Adv. Sustain. Syst.* **1**(10), 1 (2017)
36. B. Zhou, J. Song, C. Xie, C. Chen, Q. Qian, B. Han, Mo-Bi-Cd ternary metal chalcogenides: highly efficient photocatalyst for  $\text{CO}_2$  reduction to formic acid under visible light. *ACS Sustain. Chem. Eng.* **6**(5), 5754 (2018)
37. A. Saxena, W. Liyanage, J. Masud, S. Kapila, M. Nath, Selective electroreduction of  $\text{CO}_2$  to carbon-rich products by simple binary copper selenide electrocatalyst. *J. Mater. Chem. A* **6**, 4883 (2021)
38. J. Masud, W.P.R. Liyanage, X. Cao, A. Saxena, M. Nath, Copper selenides as high-efficiency electrocatalysts for oxygen evolution reaction. *ACS Appl. Energy Mater.* **1**(8), 4075 (2018)
39. A.T. Swesi, J. Masud, M. Nath, Nickel selenide as a high-efficiency catalyst for oxygen evolution reaction. *Energy Environ. Sci.* **9**(5), 1771 (2016)
40. A.D. Savariraj, V. Vinoth, R.V. Mangalaraja, T. Arun, D. Contreras, A. Akbari-Fakhrabadi, H. Valdés, F. Banat, Microwave-assisted synthesis of localized surface plasmon resonance enhanced bismuth selenide ( $\text{Bi}_2\text{Se}_3$ ) layers for non-enzymatic glucose sensing. *J. Electroanal. Chem.* **856**, 113629 (2020)
41. X. Hun, S. Wang, S. Mei, H. Qin, H. Zhang, X. Luo, Photoelectrochemical dopamine sensor based on a gold electrode modified with SnSe nanosheets. *Microchim. Acta* **184**(9), 3333 (2017)
42. J. Bergman, L. Mellander, Y. Wang, A.S. Cans, Co-detection of dopamine and glucose with high temporal resolution. *Catalysts* **8**(1), 34 (2018)
43. H. Yin, C. Zhou, C. Xu, P. Liu, X. Xu, Y. Ding, Aerobic oxidation of D-glucose on support-free nanoporous gold. *J. Phys. Chem. C* **112**(26), 9673 (2008)
44. Q. Li, S. Cui, X. Yan, Electrocatalytic oxidation of glucose on nanoporous gold membranes. *J. Solid State Electrochem* **16**, 1099–1104 (2012)
45. H.J. Qiu, G.P. Zhou, G.L. Ji, Y. Zhang, X.R. Huang, Y. Ding, A novel nanoporous gold modified electrode for the selective determination of dopamine in the presence of ascorbic acid. *Colloids Surfaces B Biointerfaces* **69**(1), 105 (2009)
46. J.Y.C. Liew, Z.A. Talib, Z. Zainal, M.A. Kamarudin, N.H. Osman, H.K. Lee, Structural and transport mechanism studies of copper selenide nanoparticles. *Semicond. Sci. Technol.* **34**(12), 125017 (2019)
47. V. Lesnyak, R. Brescia, G.C. Messina, L. Manna, Cu vacancies boost cation exchange reactions in copper selenide nanocrystals. *J. Am. Chem. Soc.* **137**(29), 9315 (2015)
48. B. Yu, W. Liu, S. Chen, H. Wang, H. Wang, G. Chen, Z. Ren, Thermoelectric properties of copper selenide with ordered selenium layer and disordered copper layer. *Nano Energy* **1**(3), 472 (2012)
49. N. Ghobadi, S. Chobin, S. Rezaee, R. Shakoury, Tuning the optical and photocatalytic features of copper selenide prepared by chemical solution deposition method. *Surfaces Interfaces* **21**(3), 100706 (2020)
50. R.D. Shannon, Revised effective ionic radii and systematic studies of interatomic distances in halides and chalcogenides. *Acta Crystallogr. Sect. A* **32**(5), 751 (1976)
51. L. Hu, C. Shang, E.M. Akinoglu, X. Wang, G. Zhou,  $\text{Cu}_2\text{Se}$  nanoparticles encapsulated by nitrogen-doped carbon nanofibers for efficient sodium storage. *Nanomaterials* **10**(2), 1 (2020)
52. A.T. Swesi, J. Masud, W.P.R. Liyanage, S. Umaphathi, E. Bohannan, J. Medvedeva, M. Nath, Textured  $\text{NiSe}_2$  film: bifunctional electrocatalyst for full water splitting at remarkably low overpotential with high energy efficiency. *Sci. Rep.* **7**(1), 1 (2017)
53. U. De Silva, J. Masud, N. Zhang, Y. Hong, W.P.R. Liyanage, M. AsleZaeem, M. Nath, Nickel telluride as a bifunctional electrocatalyst for efficient water splitting in alkaline medium. *J. Mater. Chem. A* **6**(17), 7608 (2018)
54. Y.M. Yang, J.W. Wang, R.X. Tan, Immobilization of glucose oxidase on chitosan- $\text{SiO}_2$  gel. *Enzyme Microb. Technol.* **34**(2), 126 (2004)
55. W.P. Wu, A.P. Periasamy, G.L. Lin, Z.Y. Shih, H.T. Chang, Palladium copper nanosponges for electrocatalytic reduction of oxygen and glucose detection. *J. Mater. Chem. A* **3**(18), 9675 (2015)
56. D. Ge, Y. Yang, X. Ni, J. Dong, Q. Qiu, X.Q. Chu, X. Chen, Self-template formation of porous  $\text{Co}_3\text{O}_4$  hollow nanoprisms for non-enzymatic glucose sensing in human serum. *RSC Adv.* **10**(63), 38369 (2020)